



Variations in surface ozone and carbon monoxide in the Kathmandu Valley and surrounding broader regions during SusKat-ABC field campaign: Role of local and regional sources

Piyush Bhardwaj^{1,2,*}, Manish Naja¹, Maheswar Rupakheti³, Arnico K. Panday⁴, Rajesh Kumar⁵, Khadak Mahata³, Shyam Lal⁶, Harish C. Chandola², Mark G. Lawrence³

¹Aryabhata Research Institute of Observational Sciences (ARIES), Nainital, 263002, India

²Dev Singh Bisht Campus, Kumaun University, Nainital, 263001, India

*Now at Gwangju Institute of Science and Technology (GIST), Gwangju, 61005, Republic of Korea

³Institute for Advanced Sustainability Studies (IASS), Potsdam, 14467, Germany

⁴International Centre for Integrated Mountain Development (ICIMOD), Kathmandu, 44700, Nepal

⁵National Center for Atmospheric Research (NCAR) Boulder, 80301, USA

⁶Physical Research Laboratory (PRL), Ahmadabad, 380009, India

Key words: Kathmandu, Himalayas, Air Pollution, Ozone, CO, Long Range Transport

Correspondence to: Manish Naja (manish@aries.res.in)



Highlights of the study:

- **A comparative study on trace gases among sites in the Kathmandu Valley and India.**
- 5
- **An important contribution of regional transport to the springtime ozone enhancement in the Kathmandu Valley.**
- 10
- **The winter time higher ozone levels in the Kathmandu Valley are largely due to local sources.**
- 15
- **O₃, CO and light NMHCs levels are higher in the Kathmandu Valley than the site in IGP.**
- 20
- **Regional pollution resulting from biomass burning in NW IGP led to simultaneous increase in O₃ and CO levels in the Kathmandu Valley and two sites in India.**
- 25
- **The Kathmandu Valley and the IGP have differences in their emission sources.**
- 30
- 35



Abstract

Air pollutants emitted from rapid urbanization and associated human activities in the Kathmandu Valley of Nepal over the past two decades are causing serious air quality and health concerns. These concerns led to a multinational field campaign SusKat-ABC (Sustainable atmosphere for the Kathmandu Valley-Atmospheric Brown Clouds) that measured different trace gases, aerosols and meteorological parameters in the Kathmandu Valley and surrounding regions during December 2012 to June 2013 to understand the factors influencing air quality of the Kathmandu Valley. This study provides information about the regional distribution of ozone and some precursor gases using simultaneous in situ measurements from a SusKat-ABC supersite at Bode, Nepal and two Indian sites: a high-altitude site Nainital located in the central Himalayan region and a low altitude site Pantnagar located in the Indo-Gangetic Plain (IGP). The diurnal variations at Bode showed a daytime buildup in O₃ while CO shows morning and evening peaks. Similar variations (with lower levels) were also observed at Pantnagar but not at Nainital. Several events of hourly ozone levels exceeding 80 ppbv were also observed at Bode. The CO levels showed a decrease from their peak level of above 2000 ppbv in January to about 680 ppbv in June at Bode. The hourly mean ozone and CO levels showed a strong negative correlation during winter ($r^2=0.82$ in January and $r^2=0.71$ in February), but this negative correlation gradually becomes weaker, with the lowest value in May ($r^2=0.12$). The background O₃ and CO mixing ratios at Bode were estimated to be about 14 ppbv and 325 ppbv respectively. The rate of change of ozone at Bode showed a more rapid increase (~17 ppbv/hour) during morning than the decrease in the evening (5-6 ppbv/hour), suggesting a semi urban kind of environment at Bode. The slower evening time ozone decrease rates and lower CO levels during spring suggests an important contribution of regional transport than the contribution of local sources to the springtime ozone enhancement in the Kathmandu Valley. The winter time higher ozone levels at Bode are largely due to local sources with relatively less contributions from regional sources. We show that regional pollution resulting from agricultural crop residue burning in north-western IGP led to large (~2-fold) increase in O₃ and CO levels simultaneously at all three sites, i.e., Bode, Pantnagar and Nainital during first week of May 2013. Biomass burning induced increase in ozone and related gases was also confirmed by a global model and balloon borne observations over Nainital. A comparison of surface ozone variations and composition of light non-methane hydrocarbons among different sites indicated the differences in emission sources of the Kathmandu Valley and the IGP. These results highlight the contribution of regional sources to air pollution in the Kathmandu Valley versus the local sources in the Valley.



1. Introduction

The Himalayan region is among the least studied regions in the world despite its known importance in influencing the livelihood of hundreds of millions of people and agricultural systems. The Himalayan mountain regions are spread over a large region from Afghanistan, Pakistan, India, Nepal, Bangladesh, Bhutan, China, and Myanmar, and provide fresh water to about a billion people living in this region. However, the growing economies, industrialization and increasing population in the region are polluting this pristine environment and perturbing the regional environment, climate and ecosystems. The urban centers in the mountain regions often face severe air pollution problems since the mountains act as a barrier to horizontal ventilation of the pollutants and local mountain valley winds govern the diurnal variations in air pollutants. These processes have been well studied over other parts of the world, such as Mexico City (de Foy et al., 2006; Molina et al., 2007 etc.), Po Valley (Martilli et al., 2002) and Santiago de Chile (Schmitz, 2005; Rappengluck et al., 2005). The Kathmandu Valley, located in the central Himalayas is an ideal natural laboratory to study such processes. However, only a few surface measurements of ozone and related trace species have been reported from this region (Pudasainee et al., 2006; Panday and Prinn, 2009; Christofanelli et al., 2010; Putero et al., 2015; Mahata et al., 2017).

The valley has experienced an unprecedented growth as the population increased nearly fourfold from about 0.75 million to about 3 million over the last 25 years. The total vehicle fleet in the Bagmati Zone, where the Kathmandu Valley is situated, increased by about 22 times from ca. 34,600 in 1989-90 to ca. 755,000 vehicles in 2013-14 (DoTM, 2015; <http://www.dotm.gov.np/en>). Consequently, the total fossil fuel usage in the valley is about 50% of all of Nepal. The shares of coal, petrol, diesel kerosene and liquefied petroleum gas (LPG) usage in the Kathmandu Valley



ranges between 35% and 66% when compared with their respective usage in all of Nepal (Pradhan et al., 2012). These unprecedented growths can have serious implications for the air quality and its impacts in Kathmandu Valley, such as higher occurrences of respiratory problems, skin and eye irritation have already been observed among the people living in the Kathmandu Valley than in other areas (Pradhan et al., 2012). In the past, elevated levels of O₃, CO, NO_x and VOCs have been reported over this region during winter and pre-monsoon seasons (Pudaisanee et al., 2006; Pandey and Prinn, 2009).

In order to advance our understanding of atmospheric composition in the Kathmandu Valley and surrounding broader regions, the Sustainable Atmosphere for the Kathmandu Valley- Atmospheric Brown Clouds (SusKat-ABC) international air pollution measurement campaign was carried out in Nepal during December 2012-June 2013, with an initial intensive measurement period of two months from December 2012 to February 2013 (Rupakheti et al., 2017). Eighteen international research groups participated and various instruments for the extensive measurements of aerosols, trace gases and meteorological parameters were installed. The campaign covered a total of 23 sites of various measurement capabilities in the region with a supersite at Bode, 5 satellite sites in and on the Kathmandu Valley's rim, 5 regional sites (Lumbini, Pokhara, Jomsom, Dhunche and Pyramid) and other collaborating sites in India and China, including Nainital and Pantnagar in India. Measurements of short-lived climate-forcing pollutants (SLCP) such as ozone and black carbon at Paknajol near the city center of Kathmandu during the SusKat-ABC campaign are reported in Putero et al. (2015). However, that study lacked the collocated measurements of O₃ precursors. Sarkar et al., (2016) presented the measurements of non-methane volatile organic compounds (NMVOCs) at one-second resolution using Proton Transfer Reaction-Time of Flight-



Mass Spectrometry (PTR-TOF-MS) and study on two greenhouse gases are described by Mahata et al., (2017) at Bode during the campaign. These studies provided important information about atmospheric composition in the Kathmandu Valley during the SusKat-ABC period; however, a regional picture of the atmospheric composition has not been presented so far.

5

In light of the above conditions, this study aims to provide first information about the regional distribution of ozone and related gases during the SusKat-ABC by integrating simultaneous in situ measurements of surface ozone and CO at Bode from January to June 2013 with those from two Indian sites, namely Nainital (a high altitude site in the central Himalayas) and Pantnagar (a low
10 altitude site in the Indo-Gangetic Plain (IGP)). Additional observations at the two Indian sites can also help to trace contributions of regional and local pollution. The previous measurements of ozone in the Kathmandu Valley were only performed near the city centers; however, Bode is on the eastern side of the valley and is generally downwind of the major urban centers of Kathmandu Valley (Kathmandu Metropolitan City and Lalitpur Sub-metropolitan City). This site also receives
15 regional air masses from west and south especially during afternoons with stronger wind speeds. Therefore, this site can serve as a better representative to suggest the background levels of O₃ and CO in the Kathmandu Valley, and the contribution of emissions originating from local to regional scale.

20 **2. Experimental details**

2.1. Observation sites

The Kathmandu Valley is an oval-shaped urban basin located in the central Himalayan foothills between the IGP and the Tibetan Plateau (Figure 1). The valley is surrounded by mountain peaks



with altitude ranging from 2000 to 2800 m above mean sea level (amsl) and five mountain passes (Nagdhunga, Bhimdhunga, Mudku Bhanjhyang in west, Sanga and Nagarkot in East) with altitude ranging from 1500 to 1550 m amsl and the outlet of the Bagmati River in the southwest corner of the Valley. The flat base area of the Kathmandu Valley is about 340 km² with a mean elevation
5 about 1300 m amsl. There is no river inlet into the Kathmandu Valley and only one narrow river outlet (Baghmati river) in the southwestern side. The spatial extent of the valley is about 25 km in East-West and around 20 km in the North-South direction. The measurement sites located in Kathmandu Valley during the SusKat field campaign are depicted in Figure 1b. In this study observations of O₃, CO and meteorological parameters made at Bode (27.68° N, 85.39° E, 1344 m
10 amsl) and at two sites in India viz., ARIES, Nainital; a high altitude site located on a mountain top (29.36° N, 79.45° E, 1958 m amsl) and Pantnagar; located in the Himalayan foothills in IGP (29.0° N, 79.5° E, 231 m amsl) are discussed.

2.2. Ozone and CO instruments

15 Surface measurements of ozone are made using analyzers from two make viz., Teledyne M400E (at Bode and Pantnagar) and Thermo Model-49i (at Nainital). The observation principle of both the instruments is based on the commonly used technique of attenuation of UV radiation (~254 nm) by ozone molecules. These instruments are regularly subjected to zero and span tests using internal ozone generator and ozone observations from both the instruments are also inter-compared
20 by running them side by side and using a common inlet. Further details of such inter-comparisons are reported in Sarangi et al. (2014).



CO measurements are conducted using analyzers from two make *viz.*, Horiba APMA-370 (at Bode and Pantnagar) and Thermo 48i (at Nainital). CO instrument, at Bode, was deployed for the first time in field after factory calibration from the manufacture. Nevertheless, both CO instruments were inter-compared using a common inlet prior to the campaign and correlation coefficient

5 between CO mixing ratios measured by the two instruments is estimated to be ~ 0.9 with a slope of 1.09. The detection principle of these instruments is based on commonly used method of IR absorption by CO molecules at $4.6 \mu\text{m}$. Regular zero check and span check for CO instruments are performed using a primary calibration mixture from Linde UK (1150 ppbv; Sarangi et al., 2016) and secondary gas from Chemtron Science Laboratories (1790 ppbv). Multipoint calibrations

10 (ultra-pure gases) are also carried out in different observational ranges using a zero air generator (Thermo model 1160) and a dynamic gas calibrator (Thermo model 146i) (Sarangi et al., 2014). The meteorological measurements at Bode are performed using an automatic weather station (Campbell Scientific, UK).

15 Both the O₃ and CO instruments were installed at the fourth floor of a building in Bode facing eastern side of the Kathmandu Valley (Figure 2; refer Sarkar et al., 2016 for site description). The sampling inlet for these instruments was placed at the top of the building and Teflon (TFE) tubes were used for the air intake. The O₃ and CO instruments at Nainital and Pantnagar were placed in atmospheric science building at Manora Peak [refer Sarangi et al., 2014 for site description] and

20 at the College of Basic Sciences and Humanities (CBSH), G. B. Pant University of Agriculture and Technology (GBPUAT), at Pantnagar (refer Ojha et al., 2012 for site description). Observations at Bode are in Nepalese Standard Time (NST), which is 5:45 hours ahead of GMT,



and observations at Nainital and Pantnagar are in Indian Standard Time that is 5:30 hour ahead of GMT.

2.3. Air sampling and analysis for hydrocarbons

5 Daily air samples were collected from 30 December 2012 to 14 January, 2013 at Bode, making total 16 air samples collection. These air samples are collected at 1400 hour (two samples at 1200 hour) when the boundary layer is fully evolved and the air is well mixed. Air samples are collected at a pressure of 1.5 bar and analyzed for ethane, ethane, propane, i-butane, n-butane, acetylene and i-pentane using a gas chromatograph (HP 5890 II) equipped with a flame ionization detector and
10 a PLOT column of KCl/Al₂O₃. Helium is employed as a carrier gas and H₂ & zero-air are used for flame. Air samples are also analyzed for CH₄ and CO using another GC (Varian Vista, 6000, USA) and employing a molecular sieve 13x, packed column (4 m). CO is measured by converting in to CH₄ using a Ni catalyst heated to about 325°C. Standard mixture from Intergas (International Gases & Chemicals), UK traceable to National Physical Laboratory (NPL), UK, is employed for
15 calibration of NMHCs. Gases from NIST, USA and Linde, UK are used for calibration of CH₄ and CO. More details on sample pre-concentration and calibration can be seen in Lal et al., (2008), Mallik et al., (2014) and Sarangi et al., (2016).

2.4. Satellite data, model and back-air trajectory

20 In this study, Ozone Monitoring Instrument (OMI) level-3 daily tropospheric column amount NO₂ data product OMNO2d (cloud screened at 30%) at 0.25° x 0.25° resolution is used to generate spatial maps during biomass burning period. This product is based on the radiance measurements



made by OMI instrument in visible (VIS, 405-465nm) channels, for detailed description of measurement principle refer Bucsele et al., (2013).

The surface level CO maps at $1.9^\circ \times 2.5^\circ$ spatial resolution are generated using MOZART-4/GEOS-5 simulations. The model is driven by NASA GMAO GEOS-5 meteorological fields, anthropogenic emissions based on David Streets' inventory for ARCTAS and FINN fire emissions (Wiedinmyer et al., 2011) with MOZART-4 chemical mechanism (Emmons et al., 2010). The datasets are provided by the University Corporation for Atmospheric Research (UCAR) which includes its programs, the National Center for Atmospheric Research (NCAR) and its labs. The fire locations during the spring time biomass burning are used from monthly MODIS collection 5, Level 2 (combined Aqua and Terra) global monthly fire product mcd14ml at 1 km resolution [Giglio,2010]. For this study fire locations with high detection confidence ($>80\%$) are used and detailed detection principle can be found in Giglio et al. (2003) and Justice et al., (2006).

To understand the synoptic scale atmospheric circulation and role of local and regional scale pollution in the variability of various trace species, four days isentropic back air trajectory analysis is performed using the Hybrid Single Particle Lagrangian Integrated Trajectory (HYSPLIT) model (Draxler and Hess, 1999). The model is driven by Global Data Assimilation System (GDAS) meteorological fields at $1^\circ \times 1^\circ$ spatial and 3-hour temporal resolution. In order to understand the origins of air masses, ensemble of 9 points with $\sim 0.2^\circ$ spacing surrounding Bode region at 2 km altitudes are used.



3 Results and Discussion

3.1 General Meteorology

The Kathmandu Valley is located in the central Himalayan region due north of the IGP and south of the Tibetan Plateau. The valley is influenced by the South-Asian monsoon and in general receives most of its precipitation during summer (June-September). The remaining seasons are relatively dry with spring or pre-monsoon season (March-May) being the hottest (Panday and Prinn, 2009). Figure 3 shows the diurnal variations in temperature, relative humidity (RH), solar radiation, wind speed and wind direction at Bode during January and April 2013, which are chosen as representative months for winter (Jan-Feb) and spring (Mar-May), respectively. The average daily RH during January (67%) was higher than in April (62%), with the diurnal maximum during early morning hours. During the month of January high RH in early morning hours (92% during 5-7 AM) was associated with the foggy conditions during morning hours.

The average temperature and solar radiation were higher in April (20.7° C and ~800 W/m²) than January (11.4° C and ~600 W/m²). The diurnal variations in temperature showed highest values during late afternoons which was few hours after the peak in diurnal solar radiation. The solar radiation together with the topography of Kathmandu Valley were responsible for the diurnal mountain flows in and out of the valley. The wind speeds were slowest (<1 m/s) during the night and early morning hours, primarily easterlies, and the highest wind speeds were observed during mid-late afternoon, primarily westerlies (4-6 m/s). These wind patterns were similar in both the months with April having slightly longer duration of daytime westerly flow. These wind flows, together with boundary layer dynamics are responsible for the dispersion/accumulation of pollutants during the course of a day.



The other sites in the Indian region viz., Pantnagar and Nainital also show high values of solar radiation and temperature during spring months and lowest during winter season (Ojha et al., 2012; Sarangi et al., 2014; Naja et al., 2016). The Nainital site which is at a remote mountain top and experiences moderate (2-3 m/s) northwesterly winds during most of the year with prevalence of southeasterly winds during the summer monsoon period. The Pantnagar site is situated in the vicinity of Himalayan foothills in the IGP and the similar seasonal changes in temperature, RH and solar radiation are observed (Ojha et al., 2012). In the summer monsoon season, the lowest levels of O₃ and CO are observed due to arrival of cleaner marine air masses. In winter months, slow winds, lesser ventilation and lowest boundary layer heights lead to widespread fog particularly during the first week of January.

3.2 Back Air-Trajectories

Four days, nine particles, back-air trajectories at Bode are shown for January, March, May and June (Figure 4). A very strong westerly flow is seen during winter (January) and then air-mass shows a gradual decrease of wind speed in beginning of spring (March). Air-masses approach Bode even more slowly during May and pass over parts of the IGP and the Himalayas before arriving at Bode. A dramatic change in air flow is seen from May to June as air-masses arrive mostly from the east at Bode. May and June shows very limited influences of long-range transport and air-mass is mostly within the Himalayan mountainous region with some influences from plain regions. The altitude of the air-masses suggests for greater contribution from higher heights during winter, while air-masses are shown to be trapped in lower altitude region during spring (Figure 4).



The above features for Bode are similar to those seen over Nainital and Pantnagar. The back air trajectories analysis for Nainital and Pantnagar shows that long-range transport (westerly wind) is a dominant factor during winter. However, air masses mostly circulate over the continental northern Indian region at low altitudes during spring and autumn seasons when local pollution
5 plays an important role (Kumar et al., 2010; Ojha et al., 2012; Naja et al., 2016).

3.3 Variations in ozone at Bode

The monthly (January to June) average diurnal variations in ozone at Bode are shown in Figure 5. The diurnal variations in ozone show higher levels during daytime. This daytime build-up in ozone
10 is consistently observed throughout the observation period, with relatively lesser buildup during June due to prevailing cloudy/rainy conditions. Additionally, there are only a few days of observations in June, when the campaign ended. The daytime increment in surface ozone is a typical feature of polluted sites and can be associated with daytime photochemical production of ozone from its precursors in the presence of sunlight (e.g Kleinman et al., 1994) and/or through
15 mixing of ozone rich air aloft.

The very low levels of ozone (during winter months) were observed during night-time which can be attributed to titration of O_3 by NO . The boundary layer measurement made during the campaign suggests lower heights during night time with very low ventilation coefficients during this season
20 (Mues et al., 2017). The sampling inlet for the gaseous measurements was on the rooftop about 20m from the ground level, the possibility of loss of ozone due to surface deposition in highly stratified nighttime boundary layer should be much less. Just around sunrise, a dip in ozone levels was also observed which is suggested to be due to its reaction with NO and NO_2 (which are



produced by photo-dissociation of NO_3 and N_2O_5 at sunrise). A similar dip in ozone was also reported from an urban site in India (Lal et al., 2000).

At Bode, spring time higher levels of ozone with a broader peak was observed when compared
5 with winter months, this can be attributed to the increase in incoming solar radiation which in turn increases the photochemical production of ozone. In addition to photochemical production of ozone, the boundary layer evolution during morning hours also contribute to rapid increase in ozone levels, since ozone rich air aloft gets mixed with near surface ozone depleted air (e.g Rao et al., 2003; Reddy et al., 2012) and thus increases the ozone levels. Role of air-masses (local Vs
10 regional contribution) will be discussed later in subsequent sections where differences in winter and spring variations will be clearer.

3.4 Variations in CO and Hydrocarbons at Bode

The monthly average diurnal variations in CO showed two peaks, one during morning and the
15 other in the evening hours (Figure 5). The monthly mean values of O_3 and CO with standard deviation, maximum and minimum are given in Table 1. Averages of both these gases in four time periods are also given in Table 2. Diurnal variation in CO with two peaks is a typical pattern over a polluted region and such variations have been reported at different urban sites e.g., Ahmedabad (Lal et al., 2000), Kanpur (Gaur et al., 2014), Pune (Beig et al., 2007), Santiago de Chile
20 (Rappengluck et al., 2005), Chicago (Pun et al., 2003) etc. The major sources for CO in the valley are vehicular emissions, brick kiln emissions, domestic burning of biofuels for cooking and heating, garbage burning etc. Out of these, vehicular emissions, cooking and heating occurs largely during two times a day, morning and evening and with some time differences. Additionally, the



nighttime and early morning hours are characterized by very slow wind speeds, and a shallower boundary layer along with poor mixing.

It is to be noted that CO levels during morning peaks are greater than those during evening. This could be due to the overnight/early morning accumulation of CO emissions, due to poor ventilation and lower height of the boundary layer. After attaining its maximum in the morning, CO starts to decrease. During daytime the CO emissions are countered by the boundary layer evolution and dynamic processes such as flushing of CO and other pollutants by westerly winds (Figures 1 and 3) blowing throughout the afternoon across the valley through the eastern passes. The chemical loss of CO via reaction with OH radical could also contribute slightly in showing CO lower values in the daytime.

In addition to CO, observations of VOCs made at Bode (Sarkar et al., 2016) also showed similar diurnal variations with two peaks and having their levels up to about 15 ppbv. Similar to CO, many VOCs (e.g. Acetonitrile, Benzene, Furan, etc) showed higher levels during morning, when compared to the evening peaks. We have also collected one air sample almost every day during 30 December 2012 – 14 January 2013 and analyzed them for light non-methane hydrocarbons (C₂-C₅) and for CH₄-CO. Average values along with standard deviation, minimum, maximum and number of samples are given in Table 3. Methane levels are much higher than the global average and average values of other hydrocarbons varied from about 1 ppbv to about 4.4 ppbv. The maximum value is observed to be of propane (15.48 ppbv) and acetylene (14.35 ppbv). These highest mixing ratios are observed on 7 January 2013.



The mixing ratios of methane and all these eight light non-methane hydrocarbons are much higher than those observed at Nainital (Sarangi et al., 2016) and somewhat comparable with those at Pantnagar/Haldwani (December data). Additionally, none of these sites in India show higher value exceeding 10 ppbv like those at Bode. Methane mixing ratio is also higher at Bode (2.55 ppmv) than those at Nainital (1.89 ppmv). Figure 6 shows a comparison of contribution of eight light NMHCs at Bode, Nainital, Pantnagar (including another town Haldwani) (Sarangi et al., 2016) and Kanpur (Lal et al., 2008). Bode data are for December-January months, while data from rest of three sites are in December month. Composition at Bode shows difference with those at Indian sites. Propane (20%) and n-butane (13.5%) show greater contribution, while contribution of i-pentane (4.2%) is significantly lower at Bode when compared with India sites. Greater contribution of propane and n-butane indicates for some leakages of liquefied petroleum gases (LPG) in the Kathmandu Valley.

3.5 Correlation between ozone and CO

It has been discussed in the previous section that O₃ and CO show some contrasting diurnal variations. Here we discuss about the correlation between O₃ and CO during different months (Figure 7). The highest negative correlation is seen in winter period ($r^2=0.82$ in January and $r^2=0.71$ in February) and this negative correlation reduces gradually with the lowest value in May ($r^2=0.12$). The reduction in the tendency of the negative correlation from January to May could be due to change in emission patterns and the boundary layer mixing. This is discussed further in the subsequent paragraphs. Hourly average CO levels show a systematic decrease from ~2300 ppbv in January to about 680 ppbv in June, whereas ozone shows a tendency of increase. The daytime ozone levels during spring season are slightly higher (~62 ppbv) when compared to winter (~54



ppbv). This spring time increase in ozone levels is also reported by several other studies in northern part of the Indian subcontinent (Kumar et al., 2010; Ojha et al., 2012; Kumar et al., 2013; Gaur et al., 2014). The higher values of CO during winter season can be attributed to an increase in its emissions (domestic and garbage burning to keep warm in winter season) and their inefficient dilution due to poor mixing and shallower boundary layer (Mues et al., 2017). However during 5 spring season, reduction in some of these emissions and well mixed daytime boundary layer leads to show lower CO levels.

Figure 7 shows daily variations in O₃ and CO during four different times *i.e.*, 0300-0500 hours, 10 0730-0830 hours, 1300-1500 hours, and 2200-2300 hours. It is considered that 0300-0500 hours and 2200-2300 hours would provide information for the periods when photochemical production of ozone is absent, while 1300-1500 hours can be used to understand the behavior during the periods of high photochemical activity and fully evolved daytime mixed layer. Variations during 0730-0830 hours will provide the information during morning period. The stable nocturnal 15 boundary layer just starts evolving during morning hours and air mass close to surface begins to mix with air at higher heights. In general, CO levels (blue line) show a decrease from January to June during 0300-0500 hours, 0730-0830 hours, and 2200-2300 hours, while they do not show significant changes during 1300-1500 hours. In-contrast, ozone levels (red lines) are increasing from January to May/June during all four time periods. The highest noontime ozone level is 20 observed to be about 80 ppbv during January to March that increases to about 102 ppbv during April-May. The noontime ozone level comes down to about 46 ppbv in June, which is mainly due to begin of monsoon when influence of cleaner air could be dominating.



The increase in ozone from January to May is rather more during nighttime or early morning hours, when photochemical production of ozone is absent. This suggests an enhancement in the background ozone levels. Night time values might have more influences of the daytime air mass when compared to the early morning hours. Hence, probably, average ozone value (13.1 ± 1.2 5 ppbv) during early morning period of 0300-0500 hours would represent background ozone levels for this region. However, the emissions are directly influencing the CO levels. Hence, the estimated CO mixing ratio (325.4 ± 98.3 ppbv) during noontime (1300-1500 hours) could be considered as background levels for the Bode region. Since the noontime boundary layer at Bode is assumed to be well mixed and the fast westerly flows across the valley reduces the direct 10 sampling of air-masses at Bode from its immediate emission sources scattered in the valley.

Figure 8 also shows correlation between O₃ and CO for different time periods. Weak negative correlation is seen during early morning (0300-0500 and 0730-0830 hours) or night hours (2200-2300 hours), while a slight positive correlation is seen during noon period (1300-1500 hours). In 15 general, the high altitude sites (Kaji et al., 1998; Tsutsumi and Matsueda, 2000; Naja et al., 2003; Sarangi et al., 2014) and cleaner site (e.g. Island sites, Pochanart et al., 1999) show a positive correlation between O₃ and CO.

3.6 Regional distribution of O₃ and CO during SusKat

20 Apart from O₃ and CO observations at Bode, simultaneous observations of these two gases were also made at the central Himalayan site in India (Nainital) and a site in Himalayan foothills in the IGP region (Pantnagar) and are discussed in this section (Figure 9). Average diurnal patterns in O₃ and CO are somewhat similar at Bode and Pantnagar having twin peaks in CO and daytime high



levels of O₃. However, different variations are observed at Nainital (green line), which being a remote high altitude site does not show any daytime photochemical buildup or nighttime loss in ozone. Further, the daytime ozone levels at Bode are higher than those at Pantnagar during winter season, while these are comparable during spring season. Additionally, CO levels are also higher
5 at Bode than those at Pantnagar during winter (Figure 9). A comparison of surface ozone measurements at Kanpur (India) showed a relative better agreement with Pantnagar (India) while measurement at Paknajol (Nepal) showed better agreement with Bode (Nepal) during both seasons (winter and spring) (Figure 9) indicating the differences in emission sources of Kathmandu Valley and the IGP.

10

The changes in ozone increase/decrease rates (ppbv/hour) are analyzed for all these five sites. Generally, the ozone increase/decrease rates are nearly symmetric during morning and evening at an urban site. However, it is asymmetric with slower changes occurring during afternoon/evening time at a rural or semi-urban sites (Naja and Lal., 2002). Ozone production is strongly dependent
15 on amount of precursor gases and available sunlight. On the contrary, evening time ozone loss depends mainly upon its titration with NO, apart from surface deposition. This rate of change of ozone during morning and evening hours has been used as an indicator of chemical environment (rural or urban) over a site (e.g., Naja and Lal., 2002). Below, we discuss calculated ozone increase/decrease rates.

20

Figure 10 shows that the wintertime rate of ozone increase in morning hours is much higher at Bode (about 17 ppbv/hour), when compared to Pantnagar (about 9 ppbv/hour). This suggests a rapid ozone buildup at Bode than at Pantnagar. In contrast, the ozone decrease rate is lower at



Bode (5-6 ppbv/hour) when compare to the decrease rate at Pantnagar (about 14 ppbv/hour) during spring. This suggests rather slower ozone loss at Bode via NO titration, indicating somewhat lesser polluted kind of environment in Bode during spring. However, this does not necessarily mean that NO_x emissions are lower in the Kathmandu Valley. Another process driven by diurnal variations in winds could lead to slower evening ozone loss rates. Faster afternoon westerly winds flush the pollutants out of the valley every day, leaving less NO_x to titrate ozone during evening hours. In contrast, slower winds at night allow overnight accumulation of precursor gases in nocturnal boundary layer of Kathmandu Valley that in turn can potentially contribute to next morning ozone build-up. Therefore, the slower decrease rate in evening time ozone and lower value of CO during spring, confirms somewhat lesser contribution of local pollutants in spring ozone enhancement in the valley. The regional contribution in this regard cannot be ruled out. Similar to the diurnal variations in average ozone, diurnal pattern in ozone change rates are similar at Pantnagar and Kanpur.

Back-air trajectory assisted analysis of ozone observations at Nainital in the central Himalayas show that the major role of regional/local pollution is in spring when regionally polluted ozone levels are estimated to be 47.1 ± 16.7 ppbv (Kumar et al., 2010). During spring, net ozone production over the Northern Indian Subcontinent is estimated to be 3.2 ppbv/day in regionally polluted air masses in spring but no clear build-up is seen at other times of year. While the role of long-range transport is shown to be dominating in winter with contribution of about 8-11 ppbv of ozone.



Shorter duration of solar heating during winter leads to weaker dynamical processes including convective mixing of pollutants, which in turn confines the pollutants near to the surface. Additionally, the Kathmandu Valley is isolated inside the Himalayas and the only way for pollutants to reach here is either via upslope flow of polluted air masses through the mountain valleys or arrival of polluted regional air masses from the air aloft. Thus, we feel that the wintertime higher levels of O₃ and CO at Bode are likely to be least influenced by the IGP pollution. Further similar trapping of pollutants during winter season are also reported by previous studies done over this region (Panday and Prinn, 2009). However, intense heating and stronger convective mixing could induce the IGP outflow to influence this valley region during spring season. Spring time ozone enhancement, due to IGP outflow, in the tropical marine region surrounding India has already been observed (Lal et al., 2013).

3.7 Influences of springtime northern Indian biomass burning

Every year northern Indian biomass burning emits large quantities of trace gases and aerosols and significantly affect the regional distribution of several trace species (Kumar et al., 2011; Sinha et al., 2014; Putero et al., 2014; Bhardwaj et al., 2016; Kumar et al., 2016). These studies showed the enhancement in O₃ and CO levels due to crop residue and forest fire burning in the IGP during pre- and post-monsoon seasons under favorable meteorological conditions. It has also been shown that the northern Indian biomass burning induced cooling at the surface (-27 W m^{-2}) and top of the atmosphere (-8 W m^{-2}) in the central Himalayas. This cooling leads to an additional atmospheric warming of 19 W m^{-2} (Kumar et al., 2011).

During the campaign period, simultaneous increases in O₃ and CO levels were observed at Bode, Pantnagar and Nainital (Figure 11) in the first week of May. A global model (MOZART4/GEOS5)



simulations also showed about two-fold increase in CO levels at 992 hPa in this period. Further, OMI tropospheric column NO₂ (30% cloud screened) also showed small enhancement during the same period (Figure 12). To study the possible causes, MODIS fire product and the HYPLIT back-air trajectory data are analyzed. MODIS derived fire location showed about 256% increment in
5 fire counts over the Punjab region in the IGP during 2-6 May, 2013 when compared with 28 Apr – 1 May fire counts. (Figure 12). Further, HYSPLIT 4-day back-air trajectory analysis shows that the air masses arriving at Bode were mostly circulating over Nepal region (bottom-left panel Figure 12) before the event period. However, during the high fire period the air masses were also coming from the active fire region to Bode.

10

An influence of fire activities has also been seen in the vertical profiles of ozone over the central Himalayas. Details of balloon-borne observations of ozone (Ojha et al., 2014) and meteorological parameters along with inter-comparison of two kinds of meteorological sensors (i-Met and Vaisala) are given in Naja et al. (2016). The weekly balloon borne ozone profiles made from
15 Nainital (on 9th May) also confirmed similar enhancement in ozone (~16 ppb) in the lower troposphere (2-4 km) when compared with the ozone profile on 1st May (Figure 13). The enhancement is about 14 ppbv in 4-6 km region. Such events are generally observed during the spring season, when the influence of regionally polluted air masses from the IGP could travel over long distances.

20

4. Summary

This study provides information about the regional distribution of O₃ and CO during the SusKat-ABC field campaign (Jan-Jun 2013) by analyzing simultaneous surface measurements of ozone



and CO at Bode in the Kathmandu Valley with two Indian sites, Nainital and Pantnagar. Results from few air samples and their analysis for eight (C₂-C₅) light non-methane hydrocarbons are also presented. The diurnal variations show higher levels of ozone during daytime and morning/evening peaks in CO. This daytime build-up in ozone is consistent during all months, with a relatively smaller increment during the month of June due to prevailing cloudy or rainy conditions. Such a daytime increment in surface ozone is due to the mixing of ozone rich air above the stable boundary layer and its photochemical production from precursor gases in the presence of sunlight. Very low nighttime levels of ozone were also observed during the winter season, which can be attributed to the titration of O₃ by NO. The diurnal variations in CO showed two peaks during morning and evening hours, due mainly to rush hour traffic sources and cooking activities, and such a distribution is also observed at Pantnagar. The evening peak was relatively less prominent, due to fast westerly winds blowing across the valley during daytime that flushes out CO in contrast to calm nighttime winds and a shallow nocturnal boundary layer, resulting in the highest levels being observed during morning time. After reaching its maximum levels during morning time (up to 2300 ppbv in winter months), the levels decrease as the day progresses. This decrease is attributed to the boundary layer evolution and strong winds blowing across the Valley which dilutes the CO levels. .

The correlations between O₃ and CO are found to be negative in the winter period ($r^2=0.82$ in January and $r^2=0.71$ in February) and this negative correlation becomes weaker gradually, with the lowest value in May ($r^2=0.12$). Hourly average CO levels also show a systematic decrease from its level of about 2100 ppbv in January to about 600 ppbv in June, whereas ozone shows the opposite tendency. A weaker negative correlation is observed during early morning (0300-0500



and 0730-0830 hours) or nighttime hours (2200-2300 hours) while a slight positive correlation is seen during the noon period (1300-1500 hours). The background O₃ and CO levels at Bode are found to be about 14 ppbv and 325 ppbv respectively. It is shown that O₃, CO and light non-methane hydrocarbon levels are higher at Bode than those at one of the IGP sites (Pantnagar) in the Himalayan foothills, particularly in winter. The rate of change of ozone during morning and evening hours is different at Bode, with a faster ozone increase rate during the day (about 17 ppbv/hour) but a slower ozone decrease rate (5-6 ppbv/hour) in the evening, suggesting Bode as a semi-urban site. The slower decrease rate of ozone in the evening time ozone and the lower value of CO during spring confirm a somewhat lesser contribution of local pollution in the springtime ozone enhancement in the valley, along with a contribution of regional scale pollution.

During the first week of May, simultaneous increases in O₃ and CO levels were observed at Bode, Pantnagar and Nainital. The MOZART simulations during that period also indicate about a two-fold increase in near-surface CO levels. The MODIS-derived fire location showed a ~256% increment over the Punjab region in the IGP, which could emit large amounts of precursor gases. Furthermore, during the event, the majority of air masses arriving at Nainital, Pantnagar and Bode were coming from the Punjab region. The balloon borne ozone profiles from Nainital also confirmed the significant enhancement in ozone (~16 ppbv) in the lower troposphere between the balloon flights on May 1st and 9th, 2013. Such events are mainly observed during the spring season when the influence of regionally polluted air masses from the IGP region are observed over measurement sites in the Himalayan region. This study has provided first time measurements of O₃ and CO downwind of city centers in the Kathmandu Valley. In future studies, collocated NO_x



and NMHCs measurements will be important to help understand the atmospheric chemistry better, which will be important in developing effective mitigation strategies.

Acknowledgments

5 SusKat field campaign was supported by IASS, Germany and ICIMOD, Nepal. O₃, CO and light NMHCs observations are supported by ATCTM project of ISRO-Geosphere Biosphere Program and ARIES, DST. Authors are thankful to Bhogendra Kathayat, Dipesh Rupakheti and Shyam Newar for their help in conducting observations at Bode. The IASS is supported by the German Ministry of Education and Research (BMBF) and the Brandenburg State Ministry of Science,
10 Research and Culture (MWFK). The National Center for Atmospheric Research is supported by the National Science Foundation. We are grateful to teams of OMI, MOZART and HYSPLIT for making available the respective data. Constructive suggestions from two reviewers are highly acknowledge.



References

- Beig, G., Gunthe, S., Jadhav D. B.: Simultaneous measurements of ozone and its precursors on a diurnal scale at a semi urban site in India, *J. Atmos. Chem.*, doi:10.1007/s10874-007-9068-8, 2007.
- 15 Bhardwaj, P., Naja, M., Kumar, R., and Chandola, H. C.: Seasonal, interannual and long term variabilities in biomass burning activity over South Asia, *Environ. Science and Pollution Research*, doi:10.1007/s11356-015-5629-6, 2016.
- Bucsela, E. J., Krotkov, N. A., Celarier, E. A., Lamsal, L. N., Swartz, W. H., Bhartia, P. K., Boersma, K. F., Veefkind, J. P., Gleason, J. F., and Pickering, K. E.: A new stratospheric and tropospheric NO₂ retrieval algorithm for nadir-viewing satellite instruments: applications to OMI, *Atmos. Meas. Tech.*, 6, 2607-2626, doi:10.5194/amt-6-2607-2013, 2013.
- 20 Cristofanelli, P., Bracci, A., Sprenger, M., Marinoni, A., Bonafè, U., Calzolari, F., Duchi, R., Laj, P., Pichon, J. M., Roccato, F., Venzac, H., Vuillermoz, E., and Bonasoni, P.: Tropospheric ozone variations at the Nepal Climate Observatory Pyramid (Himalayas, 5079 m a.s.l.) and influence of deep stratospheric intrusion events, *Atmos. Chem. Phys.*, 10, 6537–6549, doi:10.5194/acp-10-6537-2010, 2010.
- de Foy, B., Varela, J. R., Molina, L. T., and Molina, M. J.: Rapid ventilation of the Mexico City basin and regional fate of the urban plume, *Atmos. Chem. Phys.*, 6, 2321-2335, doi:10.5194/acp-6-2321-2006, 2006.
- 30 Draxler, R. R., Hess, G. D.: An overview of the HYSPLIT_4 modelling system for trajectories, dispersion, and deposition, *Aust. Meteor. Mag.*, 47, 295-308, 1998.



- Emmons, L. K., Walters, S., Hess, P. G., Lamarque, J.-F., Pfister, G. G., Fillmore, D., Granier, C.,
Guenther, A., Kinnison, D., Laepple, T., Orlando, J., Tie, X., Tyndall, G., Wiedinmyer, C.,
Baughcum, S. L., and Kloster, S.: Description and evaluation of the Model for Ozone and
Related chemical Tracers, version 4 (MOZART-4), *Geosci. Model Dev.*, 3, 43-67,
5 doi:10.5194/gmd-3-43-2010, 2010.
- Giglio, L., J. Descloitres, J., Justice, C. O., Kaufman Y.: An enhanced contextual fire detection
algorithm for MODIS, *Remote Sensing of Environment*, doi:10.1016/S0034-4257(03)00184-
6, 2003.
- Giglio, L.: MODIS Collection 5 Active Fire Product User's Guide Version-2.4, 2010
10 http://www.fao.org/fileadmin/templates/gfims/docs/MODIS_Fire_Users_Guide_2.4.pdf.
- Gaur, A., Tripathi, S. N., Kanawade, V. P., Tare, V., and Shukla, S. P.: Four-year measurements
of trace gases (SO₂, NO_x, CO, and O₃) at an urban location, Kanpur, in Northern India, *J.*
Atmos. Chem., 71, 283-301, doi: 10.1007/s10874-014-9295-8, 2014.
- Justice C., Giglio, L., Boschetti, L., Roy, D., Csiszar, I., Morisette J., Kaufman Y., Algorithm
15 Technical Background Document, MODIS FIRE PRODUCTS, (Version 2.3, 1 October 2006),
2006.
- Kaji, Y., Someno, K., Tanimoto, H., Hirokawa, J., Akimoto, H., Katsuno, T., Kawara J.: Evidence
30 for the seasonal variation of photo-chemical activity of tropospheric ozone: Continuous
observation of ozone and CO at Happo, Japan, *Geophys. Res. Lett.*, 25, 3505–3508, 1998.
- Kleinman, L.: Ozone formation at a rural site in the southern United State, *J. Geophys. Res.*, 99,
3469-3482, doi: 10.1029/93JD02991, 1994.



- Kumar, R., Naja, M., Venkataramani, S., and Wild, O.: Variations in surface ozone at Nainital, a high altitude site in the Central Himalayas, *J. Geophys. Res.*, 115, D16302, doi:10.1029/2009JD013715, 2010.
- Kumar, R., Naja, M., Satheesh, S. K., Ojha, N., Joshi, H., Sarangi, T., Pant, P., Dumka, U. C., Hegde, P., Venkataramani, S.: Influences of the springtime northern Indian biomass burning over the central Himalayas, *J. Geophys. Res.*, 116, D19302, doi:10.1029/2010JD015509, 2011.
- Kumar, R., Naja, M., Pfister, G. G., Barth, M. C., Brasseur G. P.: Source attribution of carbon monoxide in India and surrounding regions during wintertime, *J. Geophys. Res. Atmos.*, 118, 1981–1995, doi:10.1002/jgrd.50134, 2013.
- 25 Kumar, V., Sarkar, C., and Sinha, V.: Influence of post-harvest crop residue fires on surface ozone mixing ratios in the NW IGP analyzed using two years of continuous in-situ trace gas measurements, *J. Geophys. Res. Atmos.*, 121, 3619–3633, doi: 10.1002/2015JD024308, 2016.
- Lal, S., Naja, M., and Subbaraya B. H.: Seasonal variations in surface ozone and its precursors over an urban site in India, *Atmos. Environ.*, 34, 2713-2724, doi: 10.1016/S1352-30 2310(99)00510-5, 2000.
- Lal, S., Sahu, L. K., Gupta, S., Srivastava, S., Modh, K. S., Venkataramani, S., Rajesh T. A.: Emission characteristics of ozone related trace gases at a semi-urban site in Indo-Gangetic plain using inter-correlations., *J. Atmos. Chem.*, 60, 189-204, doi:10.1007/s10874-115-0, 2008.
- Lal, S., S. Venkataramani, S. Srivastava, S. Gupta, C. Mallik, M. Naja, T. Sarangi, Y. B. Acharya and 35 X. Liu: Transport effects on the vertical distribution of tropospheric ozone over the tropical marine regions surrounding India, *J. Geophys. Res. Atmos.*, 118, 1513–1524, doi:10.1002/jgrd.50180, 2013.



- Mahata, K. S., Panday, A. K., Rupakheti, M., Singh, A., Naja, M., and Lawrence, M. G.: Seasonal and diurnal variations of methane and carbon dioxide in the Kathmandu Valley in the foothills of the central Himalaya, *Atmos. Chem. Phys. Discuss.*, doi:10.5194/acp-2016-1136, in review, 2017.
- 5 Mallik, C., Ghosh, D., Ghosh, D., Sarkar, U., Lal, S., Venkataramani, S.: Variability of SO₂, CO, and light hydrocarbons over a megacity in Eastern India: effects of emissions and transport, *Environ. Sci. Pollut. Res.* 21: 8692. doi:10.1007/s11356-014-2795-x, 2014.
- Martilli, A., A. Neftel, G. Favaro, F. Kirchner, S. Sillman, and A. Clappier, Simulation of the ozone formation in the northern part of the Po Valley, *J. Geophys. Res.*, 107(D22), 8195, 10 doi:10.1029/2001JD000534, 2002
- Molina, L. T., Kolb, C. E., de Foy, B., Lamb, B. K., Brune, W. H., Jimenez, J. L., Ramos-Villegas, R., Sarmiento, J., Paramo-Figueroa, V. H., Cardenas, B., Gutierrez-Avedoy, V., and Molina, M. J.: Air quality in North America's most populous city – overview of the MCMA-2003 campaign, *Atmos. Chem. Phys.*, 7, 2447-2473, doi:10.5194/acp-7-2447-2007, 2007.
- 15 Mues, A., Rupakheti, M., Münkel, C., Lauer, A., Bozem, H., Hoor, P., Butler, T., and Lawrence, M.: Investigation of the mixing layer height derived from ceilometer measurements in the Kathmandu Valley and implications for local air quality, *Atmos. Chem. Phys. Discuss.*, doi:10.5194/acp-2016-1002, in review, 2017.
- Naja, M. and Lal, S.: Surface ozone and precursor gases at Gadanki (13.5°N, 79.2°E), tropical rural 20 site in India, *J. Geophys. Res.*, 107(D14), doi: 10.1029/2001JD000357, 2002.
- Naja, M., Lal, S., and Chand, D.: Diurnal and seasonal variabilities in surface ozone at a high altitude site Mt Abu (24.6° N, 72.7° E, 1680 m asl) in India, *Atmos. Environ.*, 37, 4205-4215, 2003.



- Naja, M., Bhardwaj, P., Singh, N., Kumar, P., Kumar, R., Ojha, N., Sagar, R., Satheesh, S. K., Moorthy, K. K., Kotamarthi V. R.: High-frequency vertical profiling of meteorological parameters using AMF1 facility during RAWEX–GVAX at ARIES, Nainital, *Curr. Sci.*, 111 (1) (2016), pp. 132–140, 2016.
- 5 Ojha, N., Naja, M., Singh, K. P., Sarangi, T., Kumar, R., Lal, S., Lawrence, M. G., Butler, T. M., and Chandola, H. C.: Variabilities in ozone at a semi-urban site in the Indo-Gangetic Plain region: Association with the meteorology and regional processes, *J. Geophys. Res.*, 117, D20301, doi: 10.1029/2012JD017716, 2012.
- Ojha N., Naja, M., Sarangi, T., Kumar, R., Bhardwaj, P., Lal, S., Venkataramani, S., Sagar, R.,
10 Kumar, A., Chandola, H. C.: On the processes influencing the vertical distribution of ozone over the central Himalayas: Analysis of yearlong ozonesonde observations, *Atmos. Environ.*, 88, 201–211, doi:10.1016/j.atmosenv.2014.01.031, 2014.
- Panday, A. K., and Prinn R. G.: The diurnal cycle of air pollution in the Kathmandu Valley, Nepal: Observations, *J. Geophys. Res.*, 114, D09305, doi:10.1029/2008JD009777, 2009.
- 15 Pochanart, P., Hirokawa, J., Kajii, Y., Akimoto, H., and Nakao, M.: The influence of regional scale anthropogenic activity in northeast Asia on seasonal variations of surface ozone and carbon monoxide observed at Oki, Japan, *J. of Geophys. Res.*, 104, 3621–3631, 1999.
- Pradhan, B. B., Dangol, P. M., Bhaunju, R. M., Pradhan, S.: Rapid urban assessment of air quality for Kathmandu, Nepal: Summary. Kathmandu: ICIMOD, 2012.
- 20 Pudasainee, D., Sapkota, B., Shrestha, M. L., Kaga, A., Kondo, A., and Inoue, Y.: Ground level ozone concentrations and its association with NO_x and meteorological parameters in Kathmandu Valley, Nepal, *Atmos. Environ.*, 40, 8081–8087, doi:10.1016/j.atmosenv.2006.07.011, 2006.



- Pun, B. K., Seigneur C., White W.: Day-of-Week Behavior of tropospheric Ozone in Three U.S. Cities, *Journal of the Air & Waste Management Association*, 53:7, 789-801, doi:10.1080/10473289.2003.10466231, 2003.
- Putero, D., Landi, T. C., Cristofanelli, P., Marinoni, A., Laj, P., Duchi, R., Calzolari, F., Verza, G. P., and Bonasoni, P.: Influence of open vegetation fires on black carbon and ozone variability in the southern Himalayas (NCO-P, 5079 m a.s.l.), *Environ. Pollut.*, 184, 597–604, 2014.
- Putero, D., Cristofanelli, P., Marinoni, A., Adhikary, B., Duchi, R., Shrestha, S. D., Verza, G. P., Landi, T. C., Calzolari, F., Busetto, M., Agrillo, G., Biancofiore, F., Di Carlo, P., Panday, A. K., Rupakheti, M., and Bonasoni, P.: Seasonal variation of ozone and black carbon observed at Paknajol, an urban site in the Kathmandu Valley, Nepal, *Atmos. Chem. Phys.*, 15, 13957-13971, doi:10.5194/acp-15-13957-2015, 2015.
- Rao, S. T., Ku, Jia-Yeaong., Berman, S., Zhang, K., and Mao, H.: Summertime characteristics of the atmospheric boundary layer and relationships to ozone levels over the eastern United States, *Pure Appl. Geophys.*, 160, 21-55, 2003.
- Rappenglück, B., Schmitz, R., Bauerfeind, M., Cereceda-Balic, F., von Baer, D., Jorquera, H., Silva, Y., and Oyola, P.: An urban photochemistry study in Santiago de Chile, *Atmos. Environ.*, 39, 2913–2931, doi:10.1016/j.atmosenv.2004.12.049, 2005.
- Reddy K. K., Naja, M., Ojha, N., Lal, M.: Influences of the boundary layer evolution on surface ozone variations at a tropical rural site in India, *J Earth Syst Sci* (2012) 121: 911. doi:10.1007/s12040-012-0200-z, 2012..
- Rupakheti, M., Panday, A. K., Lawrence, M. G., Kim, S., Sinha, V., Kang, S., Naja, M., Park, J., Hoor, P., Holben, B., Sharma, R., Gustafsson, Ö., Mahata, K., Bhardwaj, P., Sarkar, C., Rupakheti, D., Regmi, R., and Pandit, A., Atmospheric pollution in the Himalayan foothills:



- Overview of the SusKat-ABC field campaign in Nepal, to be submitted to Atmospheric Chemistry and Physics, 2017
- Sarangi, T., Naja, M., Ojha, N., Kumar, R., Lal, S., Venkataramani, S., Kumar, A., Sagar, R., and Chandola, H. C.: First simultaneous measurements of ozone, CO, and NO_y at a high-altitude regional representative site in the central Himalayas, *J. Geophys. Res. Atmos.*, 119, 1592–1611, doi:10.1002/2013JD020631, 2014.
- Sarangi, T., Naja, M., Lal, S., Venkataramani, S., Bhardwaj, P., Ojha, N., Kumar, R., Chandola, H. C.: First observations of light non-methane hydrocarbons (C₂–C₅) over a high altitude site in the central Himalayas, *Atmos. Env.*, Vol. 125, Part B, January 2016, Pages 450–460, <http://dx.doi.org/10.1016/j.atmosenv.2015.10.024>, 2016.
- Sarkar, C., Sinha, V., Kumar, V., Rupakheti, M., Panday, A., Mahata, K. S., Rupakheti, D., Kathayat, B., and Lawrence, M. G.: Overview of VOC emissions and chemistry from PTR-TOF-MS measurements during the SusKat-ABC campaign: high acetaldehyde, isoprene and isocyanic acid in wintertime air of the Kathmandu Valley, *Atmos. Chem. Phys.*, 16, 3979–4003, doi:10.5194/acp-16-3979-2016, 2016.
- Schmitz, R: Modelling of air pollution dispersion in Santiago de Chile, *Atmos. Environ.*, 39, 2035–2047, doi:10.1016/j.atmosenv.2004.12.033, 2005.
- Sinha, V., Kumar, V., and Sarkar, C.: Chemical composition of pre-monsoon air in the Indo-Gangetic Plain measured using a new air quality facility and PTR-MS: high surface ozone and strong influence of biomass burning, *Atmos. Chem. Phys.*, 14, 5921–5941, doi: 10.5194/acp-14-5921-2014, 2014.
- Tsutsumi, Y., Igarashi, Y., Zaizen, Y., and Makino, Y.: Case studies of tropospheric ozone events observed at the summit of Mount Fuji, *J. Geophys. Res.*, 103, 16935–16951, 1998.



Wiedinmyer, C., Akagi, S. K., Yokelson, R. J., Emmons, L. K., Al-Saadi, J. A., Orlando, J. J., and Soja, A. J.: The Fire INventory from NCAR (FINN): a high resolution global model to estimate the emissions from open burning, *Geosci. Model Dev.*, 4, 625-641, doi:10.5194/gmd-4-625-2011, 2011.

7 **Table 1:** Monthly variations in O₃ and CO over Bode during January-June 2013.

Month	Ozone (ppbv)	Max/Min (ppbv)	Daytime average ozone (1100-1700 hours)	CO (ppbv)	Max/Min (ppbv)
Jan	23.5 ± 19.9	87.1/1.4	49.8 ± 10.2	832 ± 422	2323/218
Feb	25.6 ± 20.4	95/1.2	49.9 ± 13.9	717 ± 397	2182/162
Mar	37.4 ± 23	105.9/1.2	61.8 ± 12.0	698 ± 364	2011/158
Apr	43.5 ± 26.6	116.2/1.4	67.0 ± 20.4	667 ± 372	1969/175
May	38.6 ± 21.4	111.1/1.9	55.1 ± 18.9	401 ± 213	1656/146
Jun	31.1 ± 16	68.4/1.7	46.5 ± 8.5	303 ± 85	676/166

8



9 **Table 2:** Average (avg), standard deviation (std), maximum (max), minimum (min) and daily
 10 counts of O₃ and CO values and r² values during four time periods for the entire observational
 11 period (January – June 2013).

Time period		0300-0500 hr	0730-0830 hr	1300-1500 hr	2200-2300 hr
Ozone	Avg (ppbv)	13.1	13.9	58.9	27.8
	Std (ppbv)	1.2	1.7	10.0	7
	Max (ppbv)	54.0	52.5	102.4	70.8
	Min (ppbv)	1.8	2.0	25.9	1.4
	Counts	158	158	158	158
CO	Avg (ppbv)	833.8	1103.2	325.4	626.1
	Std (ppbv)	292.6	380.3	98.3	306
	Max (ppbv)	1770.0	2430.0	910.0	1820.0
	Min (ppbv)	150.0	160.0	160.0	190.0
	Counts	159	158	159	158
R ²		0.14	0.18	0.34	0.11

12

13

14

15

16



17 **Table 3:** Average, standard deviation, minimum and maximum mixing ratios (ppbv, except for
18 CH₄, which is in ppmv) of CH₄, CO and eight (C₂-C₅) light-NMHCs from the analysis of daily air
19 sample collection from 30 December 2012 to 14 January 2013. Percentage contribution of each
20 NMHCs is also given.

Gases	Average	Standard deviation	Minimum	Maximum	% Contribution	Analysis
Methane	2.55	0.12	2.39	2.87	--	15
CO	392.5	109.3	272	588.8	--	16
Ethane	3.49	1.24	1.01	6.35	15.8	15
Ethene	2.84	2.37	0.31	9.69	12.9	15
Propane	4.41	4.14	0.44	15.48	20.0	13
Propene	1.06	0.91	0.28	3.86	4.8	13
i-Butane	2.26	1.93	0.24	7.78	10.3	13
Acetylene	4.08	3.87	0.34	14.35	13.5	14
n-Butane	2.96	1.80	0.18	5.81	18.5	14
i-Pentane	0.92	0.84	0.15	2.63	4.2	14

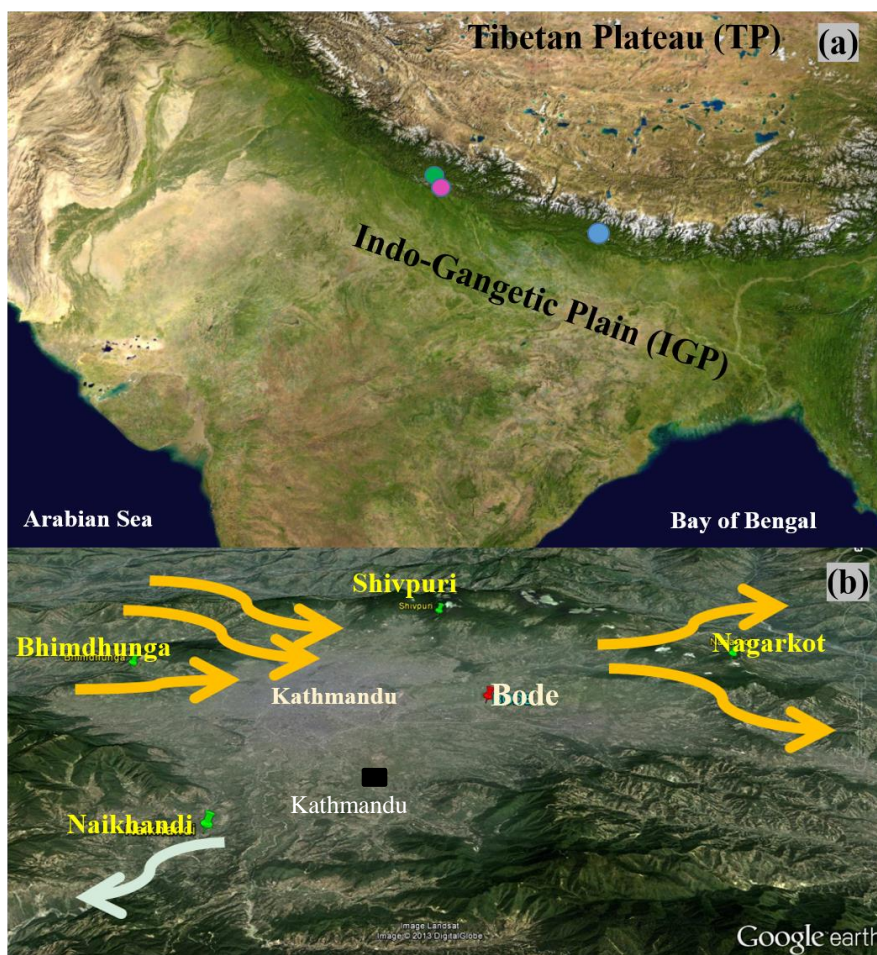
21

22

23

24

25



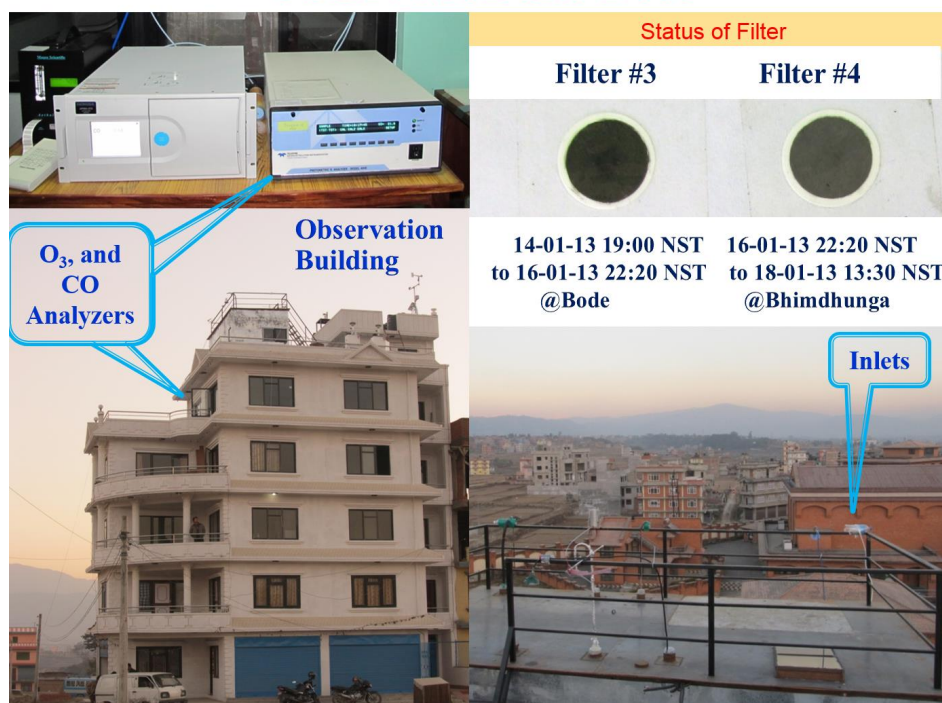
26

27 **Figure 1:** (a) Satellite image depicting the location of observation sites *viz.*, Bode (Blue) in
28 Kathmandu Valley, Nepal and Nainital (Green) and Pantnagar (Pink) in India during SusKat field
29 campaign. (b) Satellite image of the Kathmandu Valley (edge on view) with the super site (Bode)
30 and 4 satellite sites (Bhimdhunga, Naikhandi, Nagarkot, and Shivpuri). Figure (b) also indicates
31 the position of five mountain passes surrounding the valley (yellow arrows) and one river outflow
32 location (white). Kathmandu city is also marked by a black square.

33



Observation Site Bode

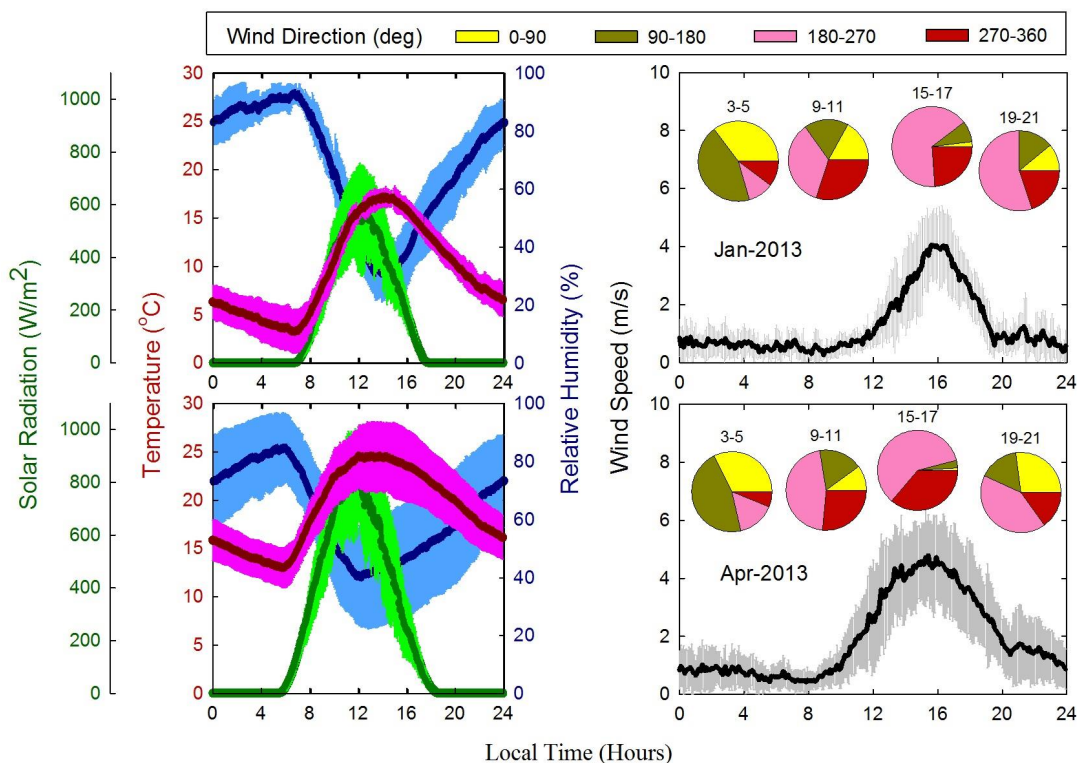


34

35 **Figure 2:** The observation setup with O₃ and CO analyzers (top-left) placed at the fourth floor in
36 a building at Bode, Nepal (bottom-left). The position of sampling inlets are towards eastern side
37 of the valley (bottom-right). Almost black inlet filters are seen in about 2 days of operations at
38 Bode and Bhimdhunga sites (top-right).

39

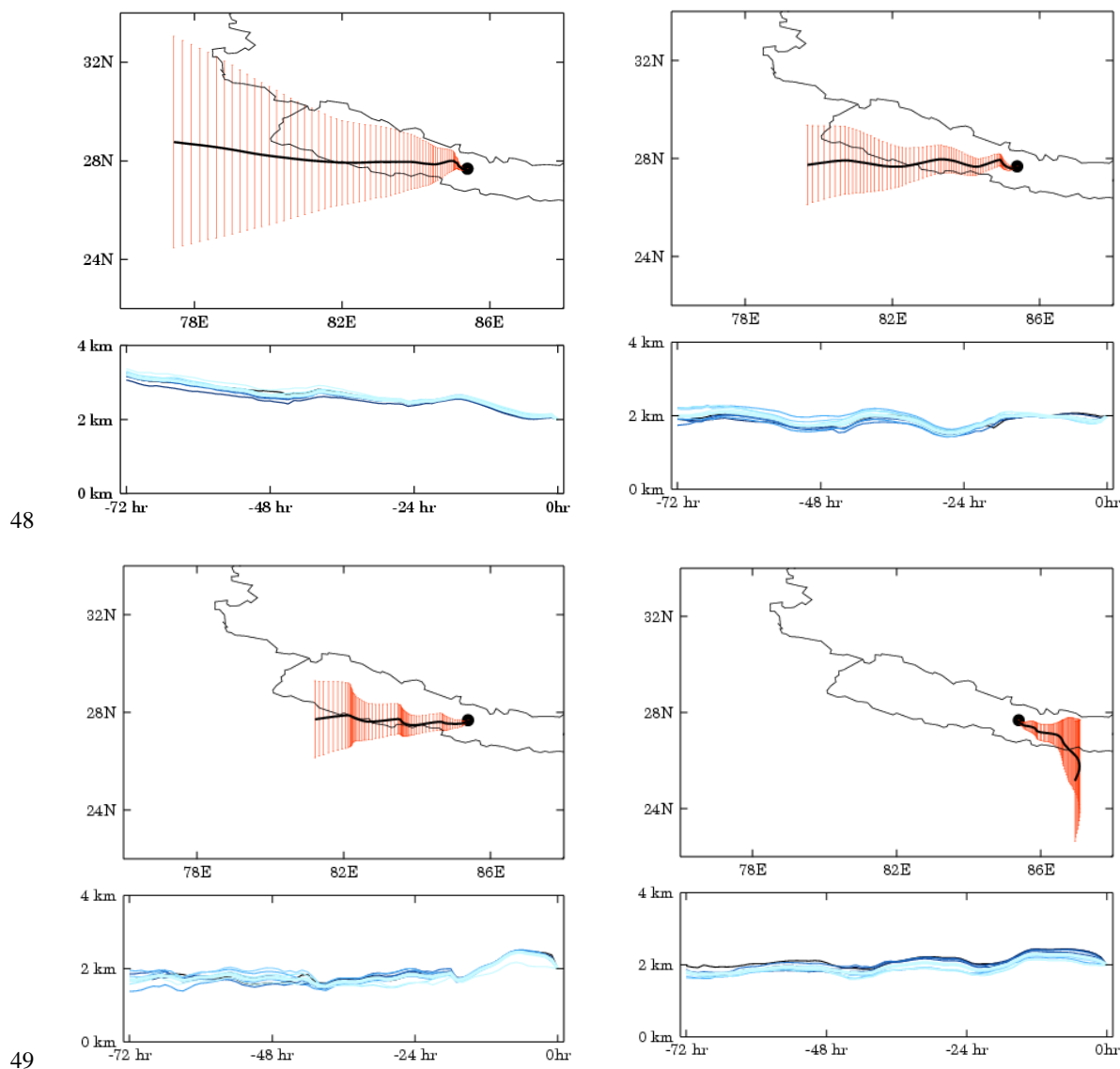
40



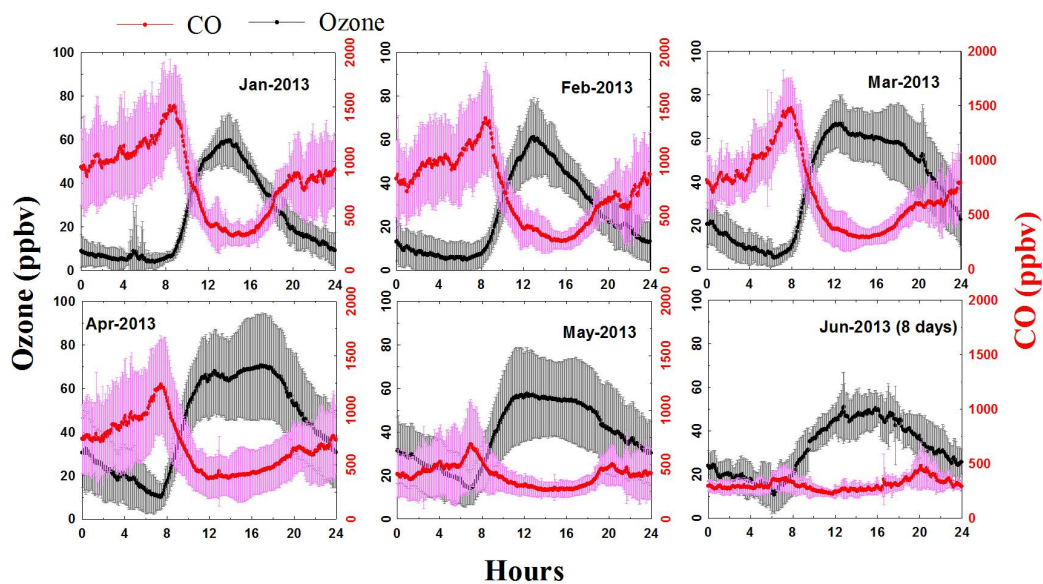
41

42 **Figure 3:** Average diurnal variations in temperature, solar radiation, relative humidity, wind speed
43 and direction at Bode during January (upper panel) and April 2013 (bottom panel). These two
44 months are taken as representative for winter and spring season respectively. (right) Wind
45 directions during four time periods (0300-0500, 0900-1100, 1500-1700 and 1900-2100 hours) are
46 shown as pie charts in wind speed plots.

47



50 **Figure 4:** Four days back-air trajectories, with a monthly average pattern using 9 particles, during
51 (a) January, (b) March, (c) May and (d) June for Bode. Altitude variations are also shown in the
52 respective lower panels.



53

54 **Figure 5:** Monthly variations in average diurnal O₃ and CO mixing ratios with 1-sigma spread at

55 Bode during January-June 2013.

56

57

58

59

60

61

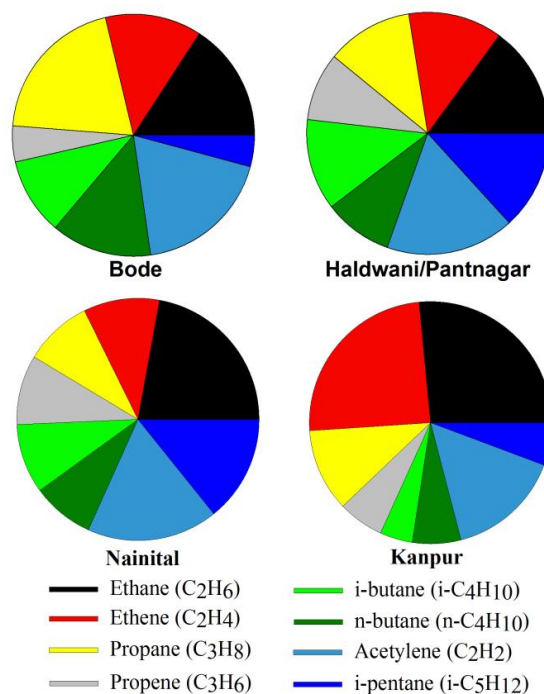
62

63

64

65

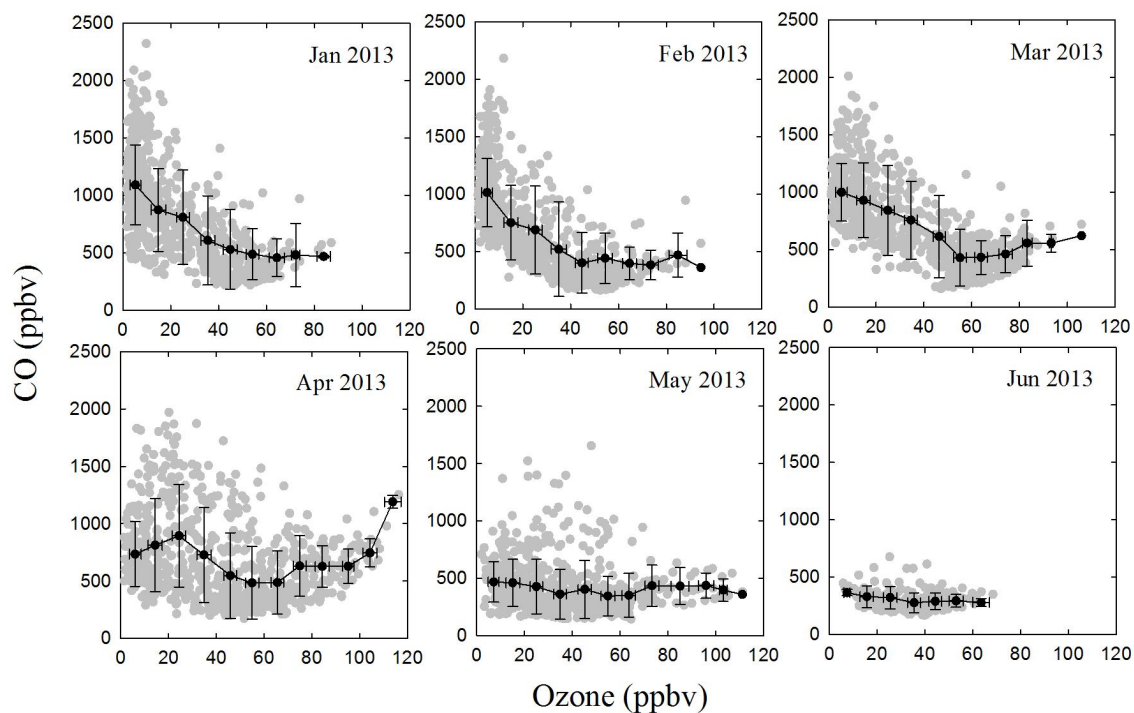
66



67

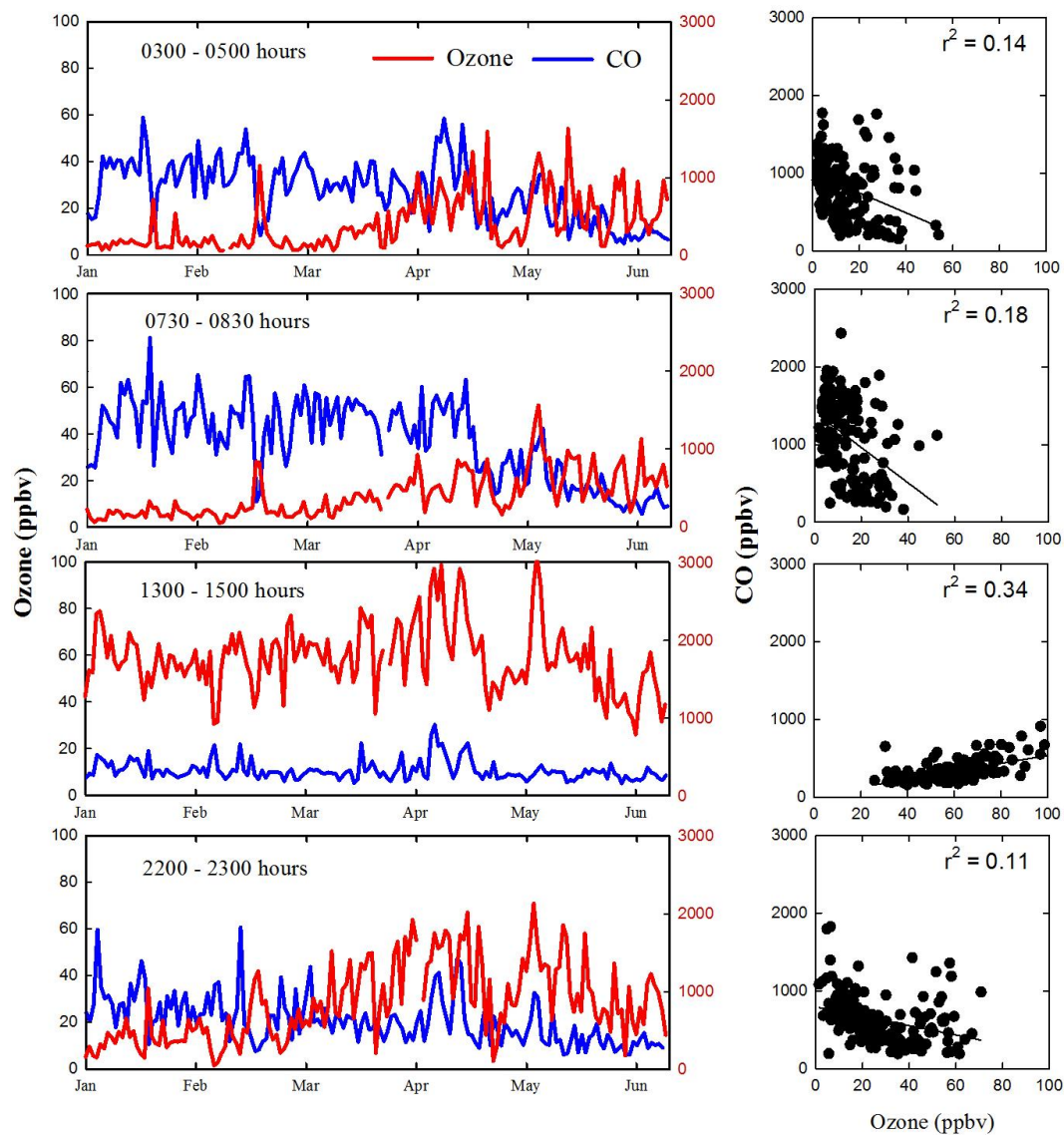
68 **Figure 6:** Contribution of eight light non-methane hydrocarbons (NMHCs) to the total NMHCs at

69 Bode, Pantnagar/Haldwani, Nainital and Kanpur in December. Bode includes January data too.



70

71 **Figure 7:** Relation between ozone and CO from January 2013 to June 2013 at Bode. Grey dots
 72 are hourly average data and black filled dots are 10 ppbv binned averaged with respect to ozone.
 73 The spread around the mean value is one sigma value.



74

75 **Figure 8:** Variations in ozone and CO during four-time periods at Bode. Correlation between
76 them is also shown (Right).

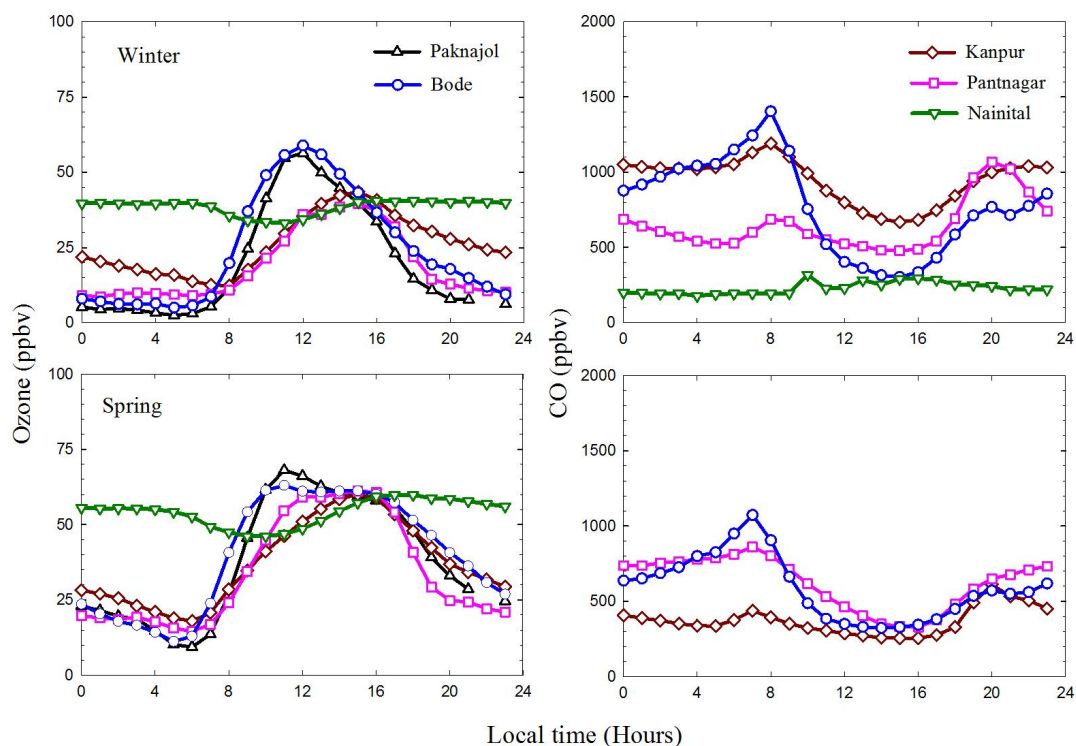
77

78



79

80



81

82 **Figure 9:** Seasonal variations in averaged diurnal ozone and CO at Bode, Pantnagar, Nainital.

83 Surface ozone observations at Kanpur (Gaur et al., 2014) and Paknajol (Putero et al., 2015) are

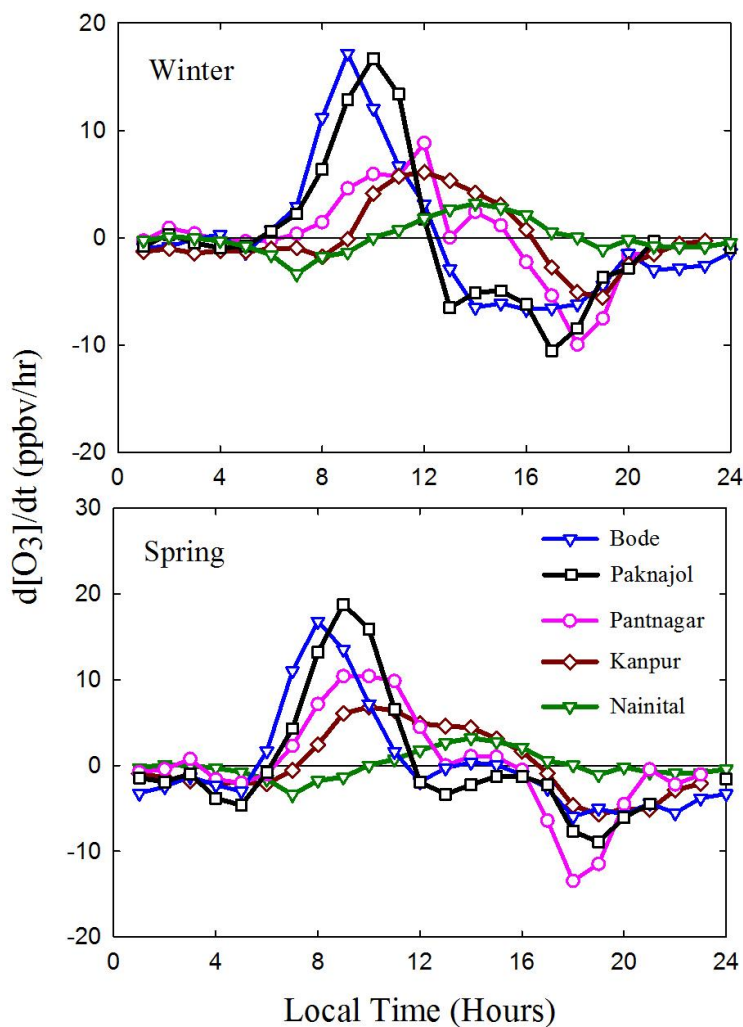
84 also shown for the comparison. CO measurements were not available at Nainital during the spring

85 season.

86

87

88



89

90 **Figure 10:** Diurnal variations in the average rate of change of ozone during winter and spring 2013
 91 at Bode (blue), Paknajol (black; Putero et al., 2015), Pantnagar (Pink), Kanpur (brown; Gaur et al.,
 92 2014) and Nainital (green).

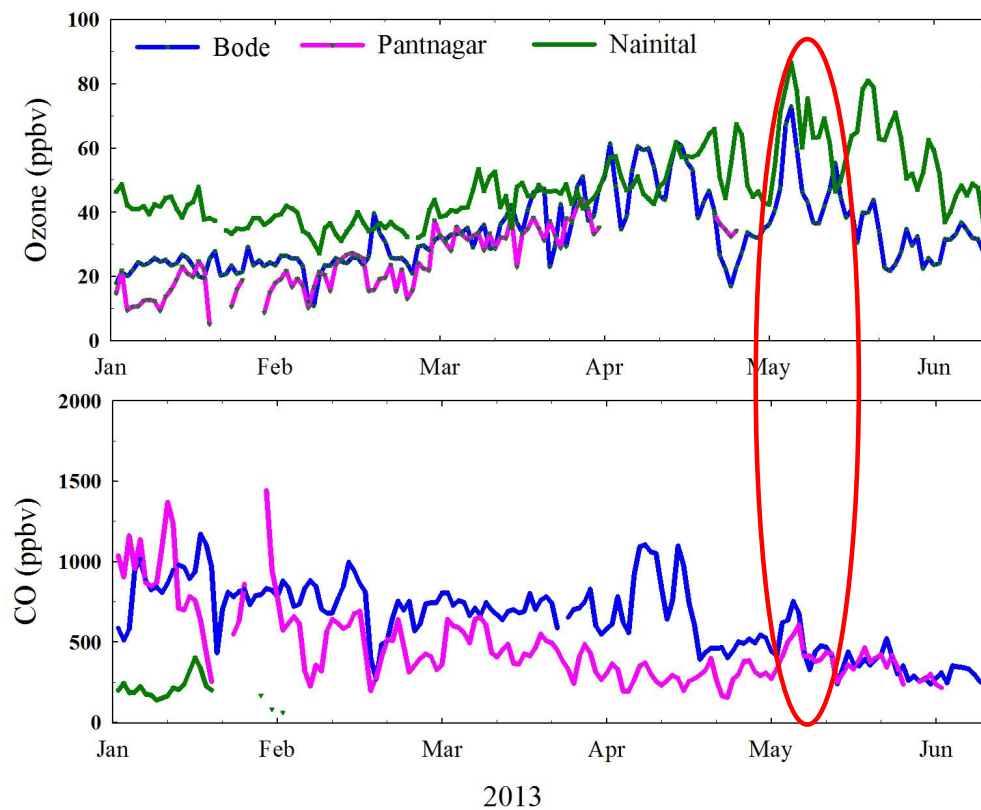
93

94



95

96



97

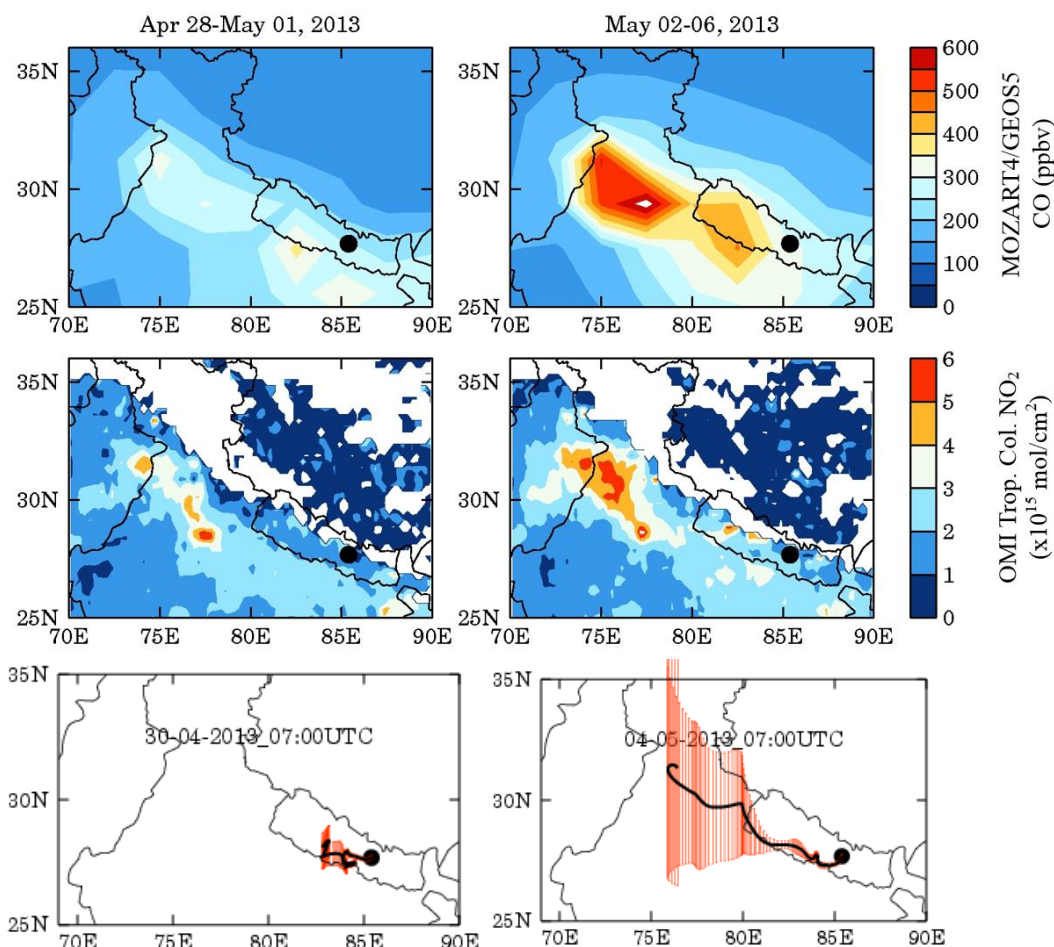
98 **Figure 11:** Time series of ozone and CO observations over the three sites viz., Bode, Nainital

99 and Pantnagar. Red oval indicates the enhancement during the first week of May.

100

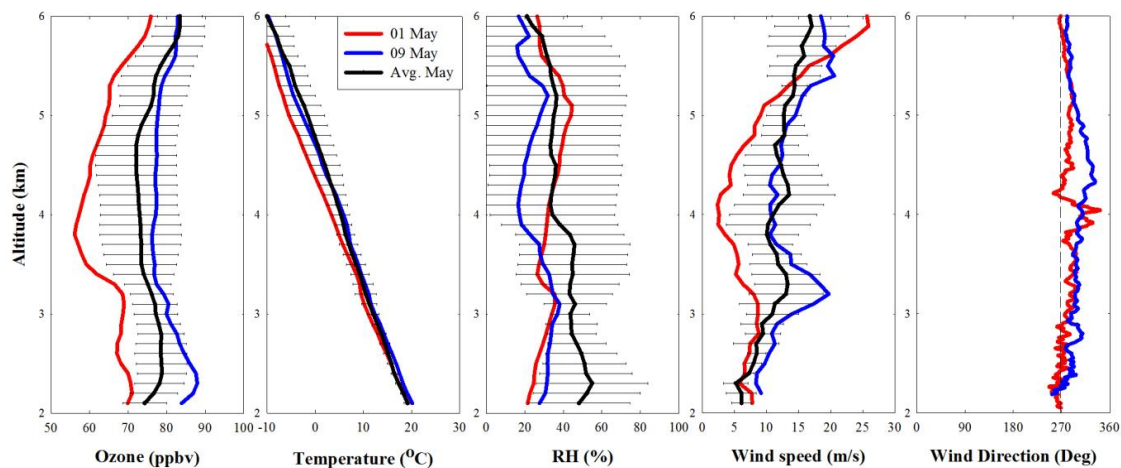


101



102

103 **Figure 12:** (Top panel) MOZART CO levels before the event period (28 Apr – 1 May 2013; left)
104 and during the event period (2-6 May 2013; right) at 992 hPa. OMI tropospheric column NO₂
105 during these two periods (Middle panels). HYSPLIT 4-day back air trajectories during April 30th
106 and May 4th 2013. Black symbol in all these figures indicates Bode supersite, Nepal.



107

108 **Figure 13:** The vertical profiles of ozone, temperature, RH, wind speed and direction over
109 Nainital region on 1st (Red) and 9th (Blue) May 2013. The black lines show respective monthly
110 average (May 2013) vertical profiles with bars representing one-sigma variations.